

# CONCURRENT EDGE AND CORNER DETECTION

<sup>1</sup>Sonya Coleman, <sup>1</sup>Dermot Kerr, <sup>2</sup>Bryan Scotney

<sup>1</sup>School of Computing and Intelligent Systems, University of Ulster, Magee, BT48 7JL, Northern Ireland

<sup>2</sup>School of Computing and Information Engineering, University of Ulster, Coleraine, BT52 1SA, Northern Ireland

## ABSTRACT

To enable fast reliable feature matching or tracking in scenes, features need to be discrete and meaningful, and hence corner detection is often used for this purpose. However, to obtain a higher level description of an image, such as identification of objects, additional information such as edges is required, and more recently detectors have been proposed that find both edges and corners. We present a combined operator, enabling edge and corner detection to be achieved concurrently. We demonstrate that accuracy is comparable to well-known existing corner detectors and edge detectors, and, as standard post-smoothing of the corner map is not required, significantly reduced computation time can be achieved.

## 1. INTRODUCTION

Many derivative-based edge detection operators have been purposed in the past 30 years, for example [2]. However, many edge detection operators are not designed to detect edge junctions and corners, and thus fail to provide edge connectivity in these areas [6]. Corners are often more abundant in real images than straight edges and are considered to be the most important features [16]; they are ideal features for tasks such as object tracking or fast interpretation of a robot's environment [6]. Corner detectors are generally developed to detect only corner points [7, 9, 10], but some have the ability to perform both as a corner detector and an edge detector [1,3,4,5,8,11,14,15,16].

A number of methods extract edges first and then determine corners as points of maximal curvature or search for points where edge segments intersect [1,4,8,16]. Thus, these methods provide both edge images and corner images that may be combined or used for different purposes [8]. However, it has been reported that the accuracy of the corner detection stage relies on the accuracy of the earlier edge detection stage, which may lead to ambiguous structure of corner points [14]. Alternative methods can work directly on the image to extract edges and corners [5,6,9,11,14,15]. Harris and Stephens [6] expanded the Moravec operator [9] to develop a combined corner and edge detector; from the corner/edge response function it may be determined if the response indicates a corner, edge, or a flat region. Smith and Brady's SUSAN corner detector [15] is based on brightness comparisons over neighbourhoods. By using different geometric threshold values the SUSAN detector can distinguish both corner and edge pixels. Shen and

Wang [14] have expanded a local edge detector so that corners may also be detected. Edges are found in a local window, and where at least two straight edges pass through a local window a corner is deemed to be present. Etou et al [5] use a modified slit rotational edge detector to detect corners. Pei and Ding [11] developed a corner detector that can also be used to detect edges and other regions of interest.

In this paper we propose an integrated edge and corner detector based on [13] that can extract edges and corners, but in which corner detection is not based directly on outputs from the edge detection. In Section 2 the framework used for the integrated detector is outlined, and performance evaluation and results obtained are presented in Section 3. The work is summarised in Section 4, and details of future research are provided.

## 2. PRODUCT OPERATOR DESIGN

In this paper we create a family of feature extraction operators, using the finite element based framework presented in [13], that can be used to detect both corners and edges concurrently but independently. In [13], near-circular Gaussian-based image derivative operators have been developed via the use of a virtual mesh and are proven to reduce angular error when detecting edges over a range of orientations. In [13] the first directional derivative  $\partial u / \partial b \equiv \underline{b} \cdot \underline{\nabla} u$  is approximated by the functional

$$E_i^\sigma(U) = \int_{\Omega} \underline{b}_i \cdot \underline{\nabla} U \xi_i^\sigma d\Omega \quad (1)$$

where  $\underline{b} = (\cos \theta, \sin \theta)$  is the unit direction. Within the functional in equation (1) the image function  $u$  is approximated by a function  $U(x, y) = \sum_{j=1}^N U_j \phi_j(x, y)$ ,

where  $\phi_i(x, y)$ ,  $i = 1, \dots, N$ , are piecewise linear basis functions defined on a triangular mesh:

$$\phi_i(x_j, y_j) = \begin{cases} 1 & \text{if } i = j \\ 0 & \text{if } i \neq j \end{cases} \quad i = 1, \dots, N; \quad j = 1, \dots, N \quad (2)$$

is associated with node  $i$ , where  $(x_j, y_j)$  are the coordinates of the nodal point  $j$ .  $\xi_i^\sigma$  is a Gaussian function defined in a neighbourhood around node  $i$  that enables Gaussian smoothing to be built into the neighbourhood operator. We extend this formulation in order to develop a combined edge and corner detector, to which we refer as

the *Linear<sup>2</sup> Gaussian operator* that also has built-in smoothing via the use of a Gaussian test function. Hence, as a corner detector, this operator does not require the additional post-smoothing that is commonplace when using corner detectors such as the Harris operator [6]. Hence a significant speed-up can be achieved, as the application of Gaussian post-smoothing carries a heavy computational burden. In order to construct this new *Linear<sup>2</sup> Gaussian* product operator, we use a first order directional derivative functional similar to that defined in equation (1), but which measures a product of the directional derivative rather than the derivative itself:

$$H_i^\sigma(U) = \int_{\Omega} (\underline{b}_i^1 \cdot \nabla U) (\underline{b}_i^2 \cdot \nabla U) \xi_i^\sigma d\Omega \quad (3)$$

Hence we now use two piecewise linear basis functions, along with a Gaussian basis function to generate the new non-linear operators  $H_{I_{xI_y}}^\sigma$ ,  $H_{I_{x^2}}^\sigma$ , and  $H_{I_{y^2}}^\sigma$ . In the case of  $H_{I_{xI_y}}^\sigma$  we choose  $\underline{b}_i^1$  and  $\underline{b}_i^2$  to be along the  $x$ - and  $y$ -coordinate directions, respectively; and for  $H_{I_{x^2}}^\sigma$  and  $H_{I_{y^2}}^\sigma$  we choose  $\underline{b}_i^1 = \underline{b}_i^2$  along the  $x$ - and  $y$ -coordinate directions, respectively. Hence we obtain directly measures of the products of directional derivatives, rather than from the product of measures of the directional derivatives. In-built smoothing is still performed via the presence of a Gaussian basis function in the operator definition. The corner strength response is then calculated as in [6], but now using the cornerness measure

$$C = \left( H_{I_{x^2}}^\sigma H_{I_{y^2}}^\sigma - (H_{I_{xI_y}}^\sigma)^2 \right) - k \left( H_{I_{x^2}}^\sigma + H_{I_{y^2}}^\sigma \right)^2 \quad (4)$$

and we choose the parameter  $k=0.04$  to be consistent with the analysis presented in [12]. Concurrently, the edge strength is calculated using the gradient magnitude that can be derived from the outputs of  $H_{I_{x^2}}^\sigma$  and  $H_{I_{y^2}}^\sigma$ . We create both  $3 \times 3$  and  $5 \times 5$  *Linear<sup>2</sup> Gaussian* product operators LLG3 and LLG5, using the near-circular virtual meshes designed in [13] and presented in Figure 1(a) and 1(b) respectively.

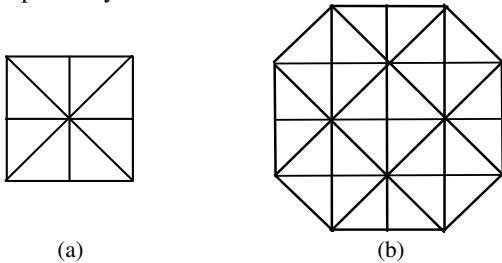


Figure 1. Triangular arrangement used for constructing the (a)  $3 \times 3$  operators; (b)  $5 \times 5$  operators

### 3. EVALUATION

We present evaluation for the product operators with respect to their performance both as corner detectors and as edge detectors. To evaluate corner detection we perform a comparative evaluation with the method of Harris [6] using the assessment methodology in [12], and for which we use the data set of synthetic corner images available at [http://www.shef.ac.uk/eee/staff/pir/Datasets-/CornerDatasets\\_f8\\_40.zip](http://www.shef.ac.uk/eee/staff/pir/Datasets-/CornerDatasets_f8_40.zip). For comparative evaluation each corner detector is applied to each image and the false positive fraction (FPF) and true positive fraction (TPF) are computed over a range of practically useful threshold values [12]. The ROC plot is generated to examine the relationship between FPF and TPF as the threshold is reduced. In accordance with [12], we have generated comparative results using the Harris operator with a Gaussian post-smoothing kernel with  $\sigma=1$ . However, as illustrated in Figure 2, we also present results for Harris using a post-smoothing kernel with  $\sigma=0.6$ , as we found this to provide improved results. It should also be noted that we have not applied non-maximal suppression to any of the algorithms, accepting the view of Rockett [12] that non-maximal suppression is merely a repair mechanism for removing detector deficiencies.

Figure 2 shows ROC plots for each corner detector. The FPF and TPF responses for LLG3 and LLG5 are comparable to Harris with  $\sigma=1$ , as further illustrated by the area under the curve (AUC), the product operators performing well as corner detectors given that no post-smoothing is required.

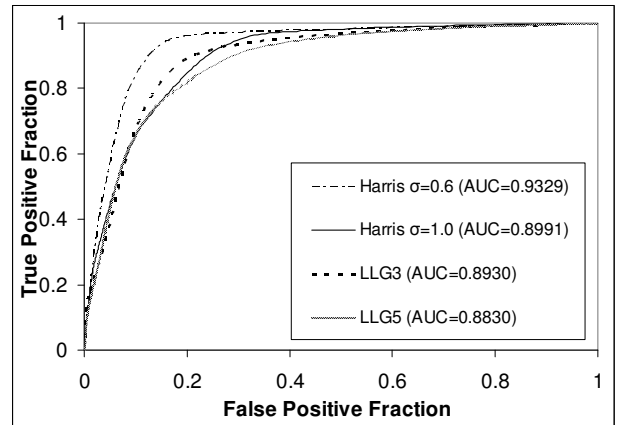


Figure 2. ROC plots for Harris corner detector and *Linear<sup>2</sup> Gaussian* operators LLG3 and LLG5

For further comparison, the visual responses from each of the corner detectors are illustrated in Figure 3; the well known block image contains 64 ground truth corners; in each case the threshold value  $T$  is selected as the visual best. A summary of the corner points detected by each method as illustrated in Figure 3 is provided in Table 1 and illustrates that the LLG5 operator detects a similar number of true corners to the Harris corner detection

methods, but with a higher number of false positives. However, the key aspect of the near-circular product operators is the absence of Gaussian post-smoothing, making them considerably more efficient in terms of reduced computational time, as can be seen from the processing times shown in Table 2.

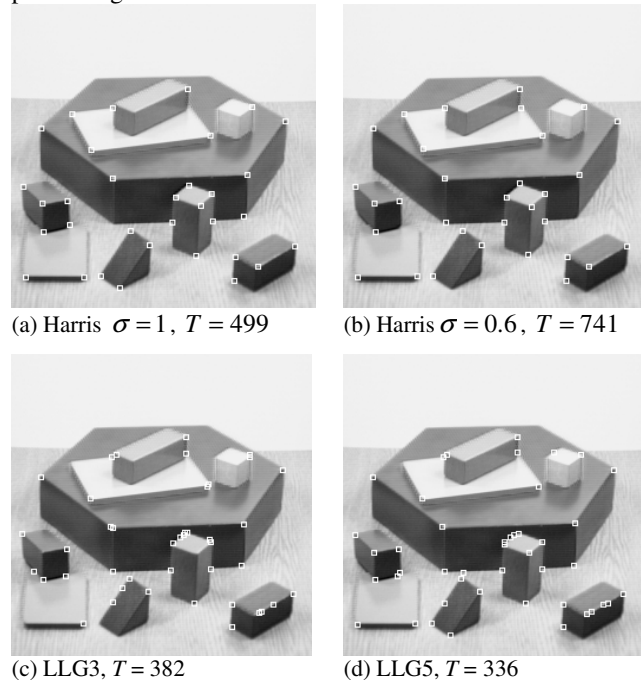


Figure 3. Illustration of detected corners for various techniques

Corner Detector	# Detected corners	# True detected corners
Harris $\sigma = 1$	33	33
Harris $\sigma = 0.6$	32	32
LLG3	38	27
LLG5	42	33

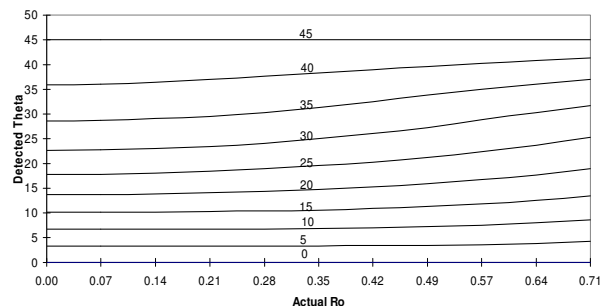
Table 1: Corner point detection rates

METHOD	Time (seconds)
Harris ( $\sigma = 0.6$ )	27.8
Harris ( $\sigma = 1.0$ )	29.5
LLG3	7.4
LLG5	13.0

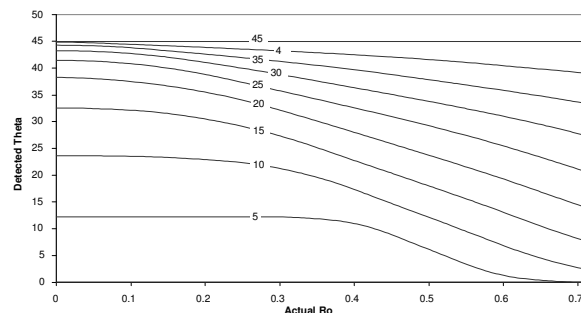
Table 2: Processing times for corner detection using the complete corner image dataset in [12]

In order to evaluate the proposed operator as an edge detector, we adopt the edge sensitivity analysis technique in [1]. The technique is used to generate edge orientation contour plots as displacement of the true edge position from the point of application of the detector is increased. Orientation  $\theta$  was sampled at  $5^\circ$  intervals over the range  $0^\circ \leq \theta \leq 45^\circ$ , so that consistency of performance over a range of actual edge angles can be assessed. Figure 4

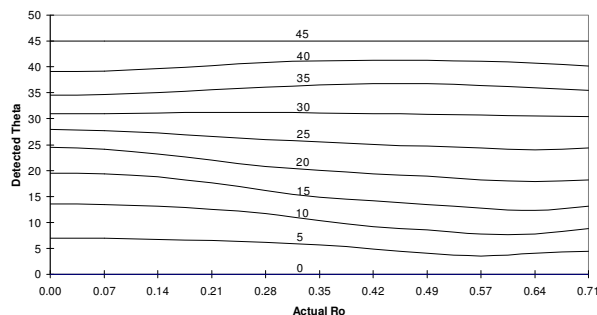
illustrates the variation in detected edge orientation  $\theta$  in relation to edge displacement  $\rho$  for Prewitt,  $5 \times 5$  Canny (C5), LLG3 and LLG5 respectively. The label on each contour shows the actual edge orientation and the units for  $\rho$  are pixels.



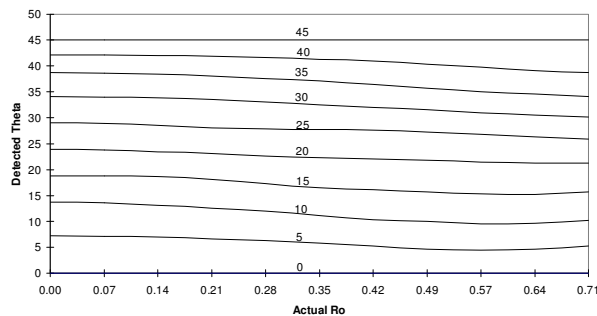
(a) Prewitt  $\theta$  Contours



(b) C5  $\theta$  Contours



(c) LLG3  $\theta$  Contours



(d) LLG5  $\theta$  Contours

Figure 4. Detected edge orientation vs displacement for operators

The contours illustrate that the product operators, LLG3 and LLG5, are comparable with the well-known Canny and Prewitt operators, with LLG5 having improved performance over LLG3. Visual comparison for the edge detection operators is provided in Figure 5 using the same image as used in Figure 3 for corner detection. Figures 5(c) and 5(d) demonstrate that the edge maps generated using the product operators contain less noise than those generated using Canny and Prewitt.

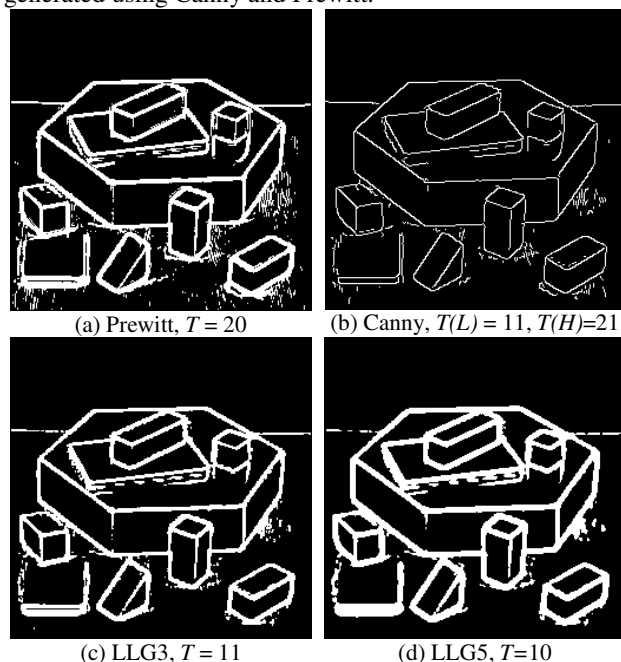


Figure 5. Edge maps for each edge detection algorithm

#### 4. SUMMARY

Feature detection plays an important role in computer vision, particularly with respect to real-time vision. We have presented a new approach, the *Linear<sup>2</sup> Gaussian* product operator, for concurrent corner and edge detection, that does not require a computationally expensive post-processing stage of applying a Gaussian smoothing kernel for corner detection. We have demonstrated the reduced computation time achieved using this method for corner detection. We have also assessed performance of the *Linear<sup>2</sup> Gaussian* product operator with respect to edge detection and illustrated that it is comparable to other well-known techniques. Future work will entail a thorough analysis to determine if the *Linear<sup>2</sup> Gaussian* product operator's performance is sufficiently accurate for feature detection when used in robot vision tasks such as navigation and localisation.

#### 5. REFERENCES

- [1] Asada, H., Brady, M., "The Curvature Primal Sketch", *IEEE Trans Pattern Analysis and Machine Intelligence*, Vol. 8, pp. 2-14, 1986.
- [2] Canny, J "Computational Approach to Edge Detection" *IEEE Trans Pattern Analysis and Machine Intelligence*, Vol. 8, No. 6, pp. 679-698, 1986.
- [3] Deriche, R., Faugeras, O.D., "2-D Curve Matching Using High Curvature Points: Application to Stereo Vision" *10<sup>th</sup> IAPR Atlantic-City*, pp. 18-23, 1990.
- [4] Deriche, R., Giraudon, G., "Accurate Corner Detection: An Analytical Study" *Proc of Int. Conf. Computer Vision* pp. 66-70, 1990
- [5] Etou, Y.; Sugiyama, T.; Abe, K.; Abe, T., "Corner detection using slit rotational edge-feature detector," *Proc IEEE ICIP*, vol.2, pp. 797- 800, 2002
- [6] Harris, C., Stephens, M., "A Combined Corner and Edge Detector" *Proc 4<sup>th</sup> Alvey Vision Conf* pp. 147-151, 1988.
- [7] Kitchen, L., Rosenfeld, A., "Gray level corner detection" *Pattern Recognition Letters*, pp.85-102, 1982.
- [8] Mokhtarian, F.; Suomela, R., "Robust Image Corner Detection Through Curvature Scale Space," *IEEE Trans on Pattern Analysis and Machine Intelligence*, vol. 20, no. 12, pp. 1376-1381, Dec 1998
- [9] Moravec, H.P., "Towards Automatic Visual Obstacle Avoidance" *Proc,5<sup>th</sup> Int. Joint Conf. Artificial Intelligence*, Cambridge, MA, USA, p584, 1977.
- [10] Noble, J.A., "Finding Corners" *Image and Vision Computing, Elsevier*, Vol. 6, No. 2, May 1988.
- [11] Pei, S.C.; Ding, J.J, "New corner detection algorithm by tangent and vertical axes and case table.", *Proc. IEEE ICIP*, vol.1, pp. I- 365-8, 11-14 Sept. 2005
- [12] Rockett, P.I., "Performance Assessment of Feature Detection Algorithms: A Methodology and Case Study on Corner Detectors" *IEEE Trans Image Processing*, Vol. 12, No. 12, pp. 1668-1676, 2003.
- [13] Scotney, B.W., Coleman S.A., "Improving Angular Error via Systematically Designed Near-Circular Gaussian-based Feature Extraction Operators" *Article in Press, Pattern Recognition, Elsevier*.
- [14] Shen, F., Wang, H., "A Local Edge Detector Used for Finding Corners" *Proc 3<sup>rd</sup> Int. Conf. Inf. Comm. and Signal Processing*, Singapore, Dec. 2001.
- [15] Smith, S.M., Brady, J.M., "SUSAN – A New Approach to Low Level Image Processing" *International Journal of Computer Vision*, Vol. 23, No. 1, pp. 45-78, 1997.
- [16] Tissainayagam, P., Suter, D., "Assessing the performance of corner detectors for point feature tracking applications" *Image and Vision Computing, Elsevier*, Vol. 22, pp. 663-679, 2004.